Hindawi Publishing Corporation
International Journal of Polymer Science
Volume 2016, Article ID 8518293, 12 pages
http://dx.doi.org/10.1155/2016/8518293

Research Article

Influence of Monomer Concentration on the Morphologies and Electrochemical Properties of PEDOT, PANI, and PPy Prepared from Aqueous Solution

Shalini Kulandaivalu,[1] Zulkarnain Zainal,[1,2] and Yusran Sulaiman[1,3]

[1]*Department of Chemistry, Faculty of Science, Universiti Putra Malaysia, 434000 Serdang, Selangor, Malaysia*
[2]*Materials Synthesis and Characterization Laboratory, Universiti Putra Malaysia (UPM), 43400 Serdang, Selangor, Malaysia*
[3]*Functional Device Laboratory, Institute of Advanced Technology, Universiti Putra Malaysia (UPM), 43400 Serdang, Selangor, Malaysia*

Correspondence should be addressed to Yusran Sulaiman; yusran@upm.edu.my

Received 19 July 2016; Revised 20 September 2016; Accepted 28 September 2016

Academic Editor: Toribio F. Otero

Poly(3,4-ethylenedioxyhiophene) (PEDOT), polyaniline (PANI), and polypyrrole (PPy) were prepared on indium tin oxide (ITO) substrate via potentiostatic from aqueous solutions containing monomer and lithium perchlorate. The concentration of monomers was varied between 1 and 10 mM. The effects of monomer concentration on the polymers formation were investigated and compared by using Fourier transform infrared spectroscopy (FTIR), Raman spectroscopy, scanning electron microscopy (SEM), cyclic voltammetry (CV), and electrochemical impedance spectroscopy (EIS) measurements. FTIR and Raman spectra showed no changes in the peaks upon the increment of the concentration. Based on the SEM images, the increment in monomer concentration gives significant effect on morphologies and eventually affects the electrochemical properties. PEDOT electrodeposited from 10 mM solution showed excellent electrochemical properties with the highest specific capacitance value of 12.8 mF/cm^2.

1. Introduction

Polymers have been well known for a long time for their excellent insulating properties. Indeed, the flow of current in the polymers was considered as unacceptable occurrence until the concept of the conducting polymers (CPs) has been reported by Shirakawa and his coworkers [1, 2] by the discovery of a conducting polymer, polyacetylene (PA). Thereby, the overall perspective of polymers has changed and gave a hike to the development of the conducting polymer. As a result, various CPs with extended π-conjugation have been developed and studied extensively. In the series of CP, poly(3, 4-ethylenedioxyhiophene) (PEDOT), polyaniline (PANI), and polypyrrole (PPy) have been the forefront of the polymer research and were chosen for this work, because of their advantageous properties.

Highlighting the interesting features, PEDOT stands out as a CP with high conductivity (ca. 300 S/cm) and exhibiting high transparency and satisfactory stability in the doped state [3, 4]. Apart from that, PEDOT shows low redox potential, low band gap (1.6–1.7 eV), and excellent chemical stability [5–7]. Despite this, substitution of ethylenedioxythiophene group at the β, β' position of the thiophene ring favours the polymerization that occurs at the α, α' position of the thiophene ring (Figure 1) resulting in the stable linear chains with fewer defects compared to the thiophene analogous [4]. In addition, the presence of the substituent containing electron-donating oxygen stabilizes the positive charge on the polymer backbone and lowers the oxidation potential of the monomer [8, 9].

In the case of PANI, it exists in different oxidation forms built from the repeating unit of benzenoid and quinoid [10]. The oxidation level varies from the fully oxidized form to reduced form classified based on the degree of polymerization [11]. Depending on the degree of polymerization, PANI appears in leuoemeraldine base (LEB), perningraniline base

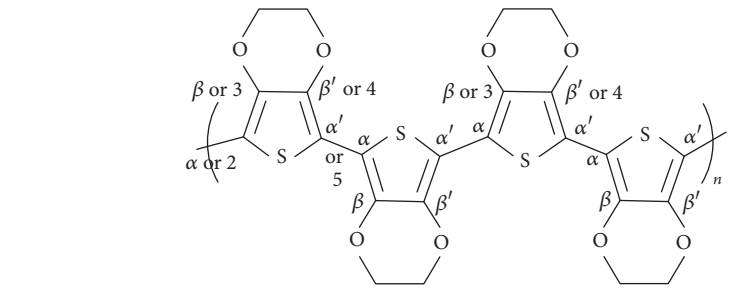

(a) Poly(3,4-ethylenedioxythiophene) (PEDOT)

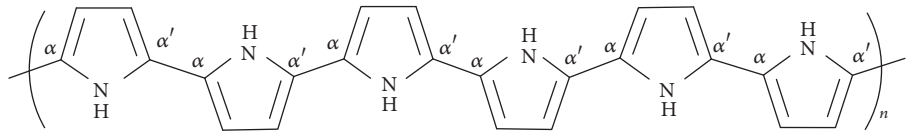

(i)

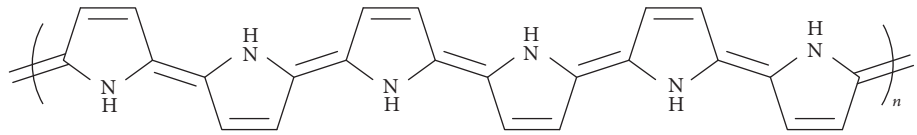

(ii)

(b) Structures of polypyrrole (PPy): (i) benzenoid form of PPy; (ii) quinoid form of PPy

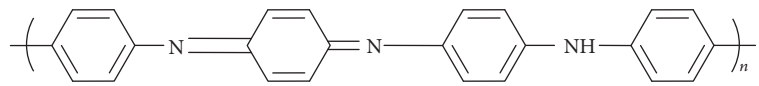

(c) Emeraldine base form of polyaniline (PANI)

Figure 1: Chemical structures of conducting polymers (a) poly(3,4-ethylenedioxythiophene) PEDOT, (b) PPy, and (c) polyaniline PANI.

(PAB), and emeraldine base (EB) forms [12]. As shown in Figure 1, EB, the conducting form of the PANI, obtained from the doping of the emeraldine salt is composed of benzenoid and quinoid ring alternatively [12, 13]. Apart from its ability to change the conductivity by adjusting the oxidation state, PANI owns several advantages, namely, good environmental stability, good electrical conductivity, and thermal stability (250°C) [14, 15].

Whereas PPy is made up from repeating unit of pyrrole ring structures creating extended π-conjugated backbone long chain [16], the long π-conjugated chain could appear in the form of aromatic or quinoid structure [17] as shown in Figure 1. PPy has excellent features including high conductivity, excellent environmental stability, good redox reversibility, and ease of synthesis [18, 19].

Reviewing the literature, most of the research interests on these homopolymers were focused on the electrochemical polymerization [20–22] due to its ease of synthesis and reproducible properties [23, 24]. In this present study, potentiostatic electrochemical polymerization method was used to investigate and compare the physical and electrochemical properties of PEDOT, PANI, and PPy film which were prepared in aqueous solution at different concentrations. Indeed, there are studies reported on electrochemical polymerization of these monomers in aqueous or nonaqueous media. However, most of the electrochemical polymerization of EDOT is attempted in organic media due to the low solubility of EDOT monomer (2.1 g/l at 20°C) in the aqueous solution [25]. Normally, polymerization of ANI is performed in acidic media [26, 27] and, to the best of our knowledge, polymerization of ANI in neutral or basic media is very limited. However, water is still an appropriate choice for the polymerization media considering the environmental concern and economical issue. Thus, this is the key factor to study in detail the electropolymerization of these monomers in aqueous solution.

2. Experimental

2.1. Chemical/Materials. 3,4-Ethylenedioxythiophene (EDOT, 97.0%), pyrrole (Py), lithium perchlorate ($LiClO_4$, 95.0%), potassium ferricyanide, $K_3Fe(CN)_6$, and potassium ferrocyanide, $K_4Fe(CN)_6$, were purchased from Sigma-Aldrich while aniline (ANI) and potassium chloride (KCl) were obtained from the Fisher Scientific. ANI and Py were freshly distilled prior to use while EDOT was used without any further purification. All these chemicals were stored in a fridge at 4°C prior to use. All the other chemicals were used as received. Indium tin oxide (ITO) coated glass was purchased from Xin Yan Technology Limited.

2.2. Instrumentation. All the electrochemical measurements were performed using a computer-controlled potentiostat/galvanostat (Autolab 101, NOVA 1.9.16,) at room temperature. PerkinElmer Fourier transform infrared (FTIR) spectrometer equipped with universal attenuated total reflectance (UATR) accessory was used to study the composition of the films. The Raman spectra of the films were recorded on Alpha300 R microscopic confocal Raman spectrometer (WITec GmbH) equipped with a 633 nm laser line. Surface morphology of the films was determined via scanning electron microscope JEOL JSM 6400 and Leo 1455 VP-SEM model.

2.3. Potentiostatic Electropolymerization. The thin films were prepared potentiostatically onto ITO glass from aqueous solution containing monomer (EDOT, ANI, or Py) in the presence of 0.1 M $LiClO_4$ supporting electrolyte at the deposition potential of 1.0 V versus Ag/AgCl/3 M. Here, three different concentrations of monomers (1, 5, and 10 mM) were studied. All the electropolymerization processes were performed in one compartment containing three electrodes placed in a Faraday cage to avoid electromagnetic field effect. The cell arrangement consists of a working electrode which was ITO coated glass with a fixed deposition area (1 cm^2), a platinum wire as a counter electrode, and Ag/AgCl as a reference electrode. The working electrodes (ITO glass) were cleaned ultrasonically in acetone followed by ethanol and finally in distilled water for 15 min each. The deionized water (resistivity ~18.2 MΩ cm) was used as a solvent to prepare all the solutions.

3. Results and Discussion

3.1. Potentiostatic Electropolymerization of EDOT, ANI, and Py. Electropolymerization of EDOT, ANI, and Py were carried out potentiostatically at fixed applied potential (E_p) of 1.0 V for 300 seconds in a solution containing monomer and 0.1 M $LiClO_4$ as supporting electrolyte. The concentration of monomer in the solution was varied (1, 5, and 10 mM) for each experiment. The PEDOT films on the surface of the indium tin oxide (ITO) glass were transparent "sky blue" which is in agreement with the reported literature [28], whereas thin transparent greenish PANI film layer and black PPy film layer were electrodeposited onto the ITO substrate, respectively.

The chronoamperograms of the PEDOT electropolymerized at different concentrations (Figure 2(a)) revealed that increasing the concentration of the monomer gives rise to the current. This could be due to the increment of the rate of the electropolymerization of the monomer to become polymer. Similar behaviour was also observed for PANI (Figure 2(b)) and PPy (Figure 2(c)). A comparable result has been reported by the Sadki and Chevrot [29] in their studies for the electropolymerization of EDOT in the presence of sodium dodecyl sulphate (SDS) and acid perchloric in methanol-water medium. Furthermore, during the experiments it has been noted that at higher monomer concentration (e.g., 10 mM) the polymer films were electrodeposited with good adherence on the working electrode surface. This result indicates that the monomer is more easily electropolymerized at a concentrated solution.

It was noticed from the chronoamperogram (Figure 2(a)) that there is an increase in the current creating a shoulder peak for 10 mM PEDOT (region (ii)) indicating the nucleation point where the formation of the nuclei on the electrode surface occurs [30]. A similar phenomenon was also observed in 5 mM and 10 PANI and PPy (Figures 2(b) and 2(c)). However, the 1 mM PEDOT and 5 mM PEDOT chronoamperograms display increment in current with the absence of nucleation peak followed by a plateau. This is the point where the first polymer nuclei form (formation of first active sites) due to the radical coupling and formation of oligomers chain [31, 32].

In contrast to PEDOT and PPy, chronoamperograms of PANI exhibit a drop in current at the initial stage indicating the adsorption and diffusion of ions onto the substrate. It should be noticed that chronoamperograms for 10 mM ANI were well defined with pronounced peak current which corresponds to the nucleation of the ANI. This observation indicates that the PANI with better adherence will be formed from the solution containing high concentrations of monomer. Whereas, the absence of increment of current for 1 mM PANI indicates that no further nucleation process has occurred or the polymer growth is stopped at the oligomer stage [30, 33], a similar observation was noticed for 1 mM PPy (Figure 2(c)). These results imply that the use of low concentration of monomer would not be a good choice for electropolymerization of the monomer on ITO substrate. However, here it is worth mentioning that, at a high monomer concentration (>10 mM), the monomers do not dissolve fully in aqueous solution limiting the concentration factor.

As illustrated in Figure 2, the electropolymerization of these polymers favours the progressive nucleation (PN) instead of instantaneous nucleation (IN) when the monomer concentration increases from 1 mM to 10 mM. IN describes the formation of nuclei at the initial stage whereas PN explains the continuous process of formation of nuclei during the polymerization process. As explained earlier, the increment of concentration induced the formation of nuclei. Thus, based on the current study, it shows that as the concentration increases from 1 mM to 10 mM, the rate of formation of nuclei increases which increases the growth rate [34].

3.2. Structural Studies

3.2.1. Fourier Transform Infrared (FTIR) Spectroscopy. Figure 3 illustrates FTIR spectra of PEDOT, PANI, and PPy prepared from various monomer concentrations and the assignments are tabulated in Table 1. The bands at 1627 cm^{-1} and 1510 cm^{-1} for PEDOT are assigned to asymmetrical and symmetrical C=C stretching vibration of the thiophene ring unit, respectively [35, 36]. The vibration at 1300 cm^{-1} is due to C-C in ring stretching of the thiophene rings [36]. The vibration modes at 1140 cm^{-1} and 1048 cm^{-1} are the indication for ethylenedioxy group stretching and C-O-C stretching of thiophene ring, respectively [36, 37]. The peaks for C-S-C deformation were noticed at 928 cm^{-1} and 761 cm^{-1} [37, 38].

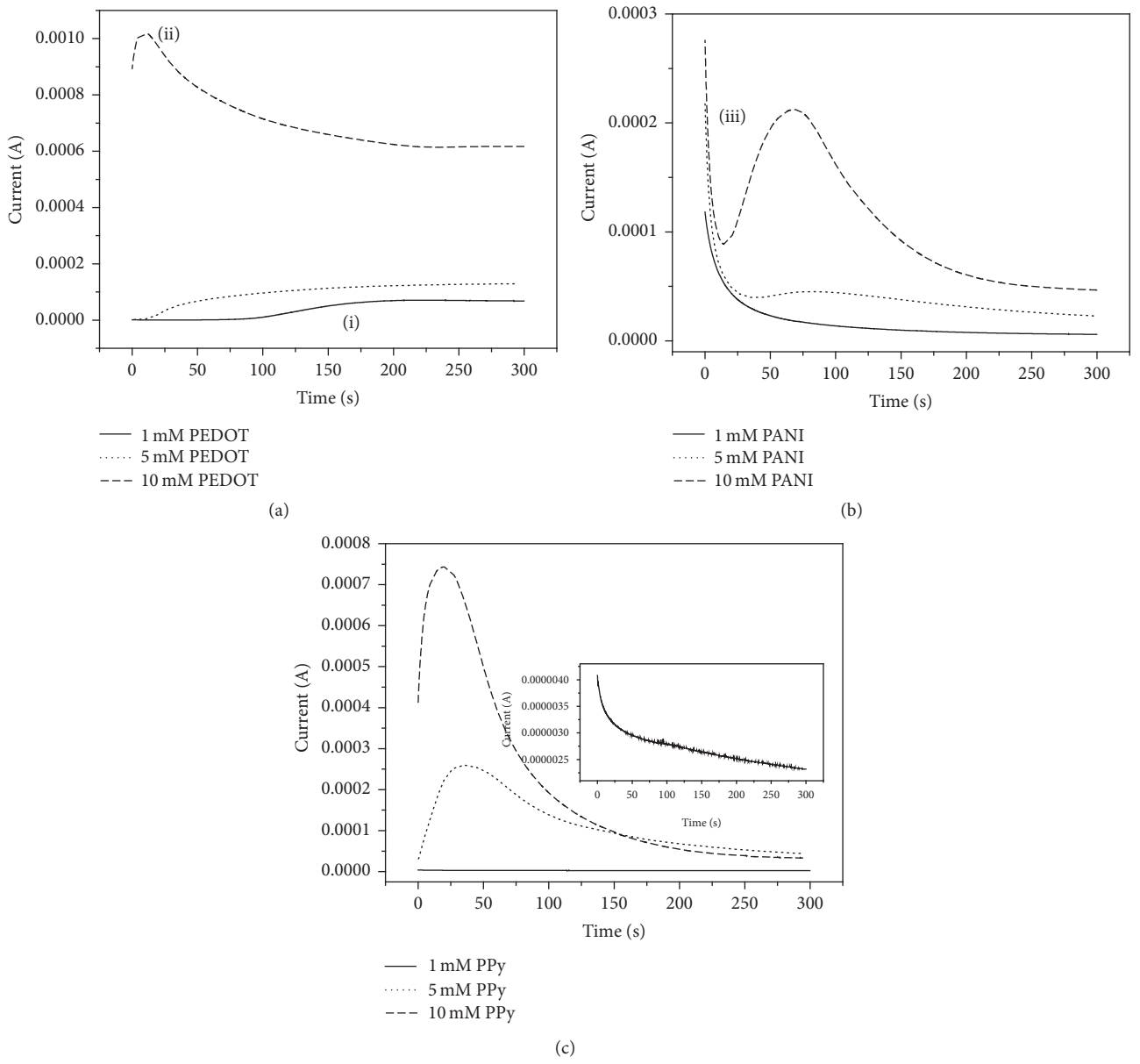

Figure 2: Chronoamperograms of (a) PEDOT, (b) PANI, and (c) PPy films electropolymerized on ITO substrate prepared from 1 mM, 5 mM, and 10 mM monomer in 0.1 M $LiClO_4$ at 1.0 V. Inset: (c) magnification of chronoamperogram of PPy prepared from 1 mM monomer.

However, the bands at 1532 cm^{-1} and 1628 cm^{-1} in PANI spectrum are associated with C=C stretching of the quinoid ring and benzenoid rings in PANI structure, respectively. However, the spectra for 1 mM and 5 mM PANI (not shown) did not exhibit any bands signifying stretching of C=C benzenoid rings, indicating ANI did not polymerize to PANI. A band at 1450 cm^{-1} is assigned to benzene structure of PANI [39]. Despite that, C-N stretching of secondary aromatic amine is observed at 1310 cm^{-1}. The peak at wave number 1090 cm^{-1} represents the vibration for C-H in-plane bending of the aromatic ring, which confirms the benzene rings are bonded at the position 1,4 in the polymer chain [40]. The bands at the region 700 cm^{-1} to 900 cm^{-1} are attributed to bending vibration of C-H out of the plane.

The FTIR spectra of PPy show bands at 735 cm^{-1} and 900 cm^{-1} attributed to stretching vibration of =C-H out of the plane. Bands at about 1643 cm^{-1} and 1532 cm^{-1} are due to C-C stretching vibration of asymmetrical and symmetrical mode, respectively [41]. However, according to spectra for 1 mM PPy (Figure S1 in Supplementary Material available online at http://dx.doi.org/10.1155/2016/8518293), no C-C stretching vibration was observed. The absence of this band in the region between 1400 cm^{-1} and 1700 cm^{-1} is evidence for a deficiency of electropolymerization process of pyrrole at the 1 mM monomer solution. Additionally, C-H in-plane stretching vibrations are seen at the position 1300 cm^{-1}. The bands at 1364 cm^{-1} and 1100 cm^{-1} are the characteristics bands for C-N stretching and N-H in-plane deformation, respectively

Table 1: FTIR assignments for the main vibrations of the PEDOT, PANI, and PPy films.

Vibrational wavenumbers (cm^{-1})			Assignments
PEDOT	PANI	PPy	
761, 928			C-S-C deformation
1140			Ethylenedioxy group deformation
1048			C-O-C stretching
1627			C=C (asymmetrical)
1510			C=C (symmetrical)
1300			C-C
	1542, 1628		C=C stretching
	1310		C-N stretching of secondary aromatic amine
	1200		
	1090		C-H in-plane bending of aromatic
	700–900		C-H out-of-plane deformation
		1643	C-C stretching (asymmetrical)
		1532	C-C stretching (symmetrical)
		1300	C-H in-plane stretching
		1364	C-N stretching
		1100	N-H in-plane deformation
		600–900	=C-H out of plane

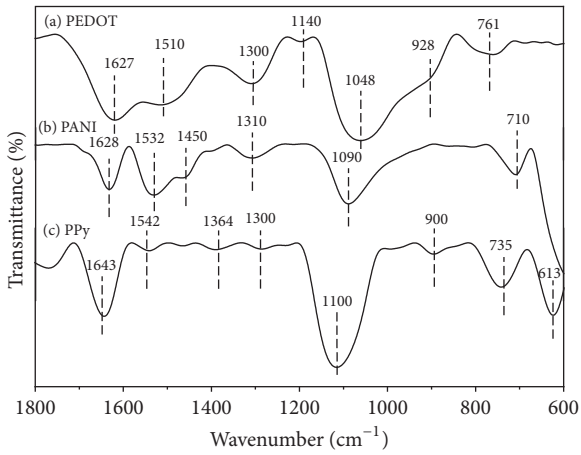

Figure 3: The FTIR-ATR spectra of (a) PEDOT, (b) PANI, and (c) PPy obtained from solution containing 10 mM monomer and 0.1 M $LiClO_4$.

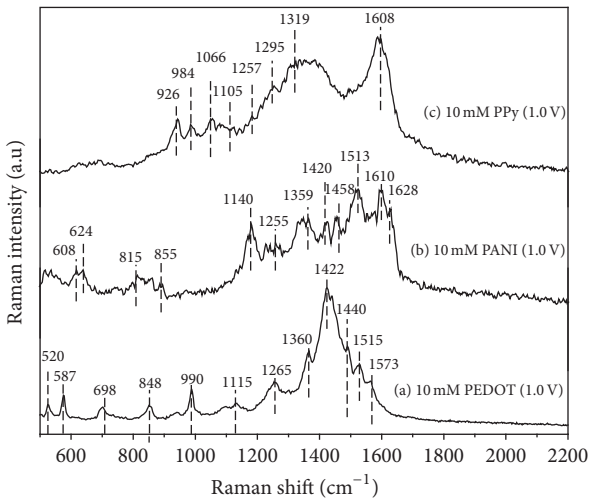

Figure 4: Raman spectra for (a) PEDOT, (b) PANI, and (c) PPy films electropolymerized at 1.0 V in 10 mM monomer containing 0.1 M $LiClO_4$.

[42]. FTIR studies show that the homopolymers were already formed after 300 seconds of electropolymerization at 1.0 V in an aqueous solution containing 10 mM monomers.

3.2.2. Raman Spectroscopy. Raman spectroscopy is used as the complementary to FTIR. PEDOT spectrum (Figure 4(a)) reveals a strong and intense band at 1422 cm^{-1} and 1440 cm^{-1} which is attributable to the symmetrical C_α=C_β stretching mode. The asymmetric C_α=C_β stretching mode was noticed at 1515 and 1573 cm^{-1}. Additionally, bands at 1115, 1265, and 1360 cm^{-1} are assigned to C-O-C ring deformation, C_α-$C_{\alpha'}$ interring stretching, and C_β-$C_{\beta'}$ stretching, respectively, whereas few weak bands were also observed at 520, 587, 848, and 990 cm^{-1} which denoted the oxyethylene ring deformation (Table 2). In addition, a single peak observed at the position of 698 cm^{-1} represents the symmetrical C_α-S-$C_{\alpha'}$ ring deformation [43]. Additionally, an important noteworthy feature in the Raman spectrum is the absence of peaks in the region 650 cm to 680 cm which indicates the resultant PEDOT polymer is in a planar structure [30].

The Raman spectrum of PANI (Figure 4(b)) illustrates three main frequency regions which determine the characteristics of the polymer as reported by Mažeikiene et al. [44]. A band at 1628 cm^{-1} is originated from the stretching vibrations

Table 2: Assignments of the Raman bands for the PEDOT, PANI, and PPy.

Vibrational wavenumbers (cm^{-1})			Assignments
PEDOT	PANI	PPy	
520, 587, 848, 990			Oxyethylene ring deformation
698			C_α-S-$C_{\alpha'}$ ring deformation
1115			C-O-C ring deformation
1265			C_α-$C_{\alpha'}$ interring stretching
1360			C_β-$C_{\beta'}$ stretching
1422, 1440			Symmetric C_α=C_β (stretch)
1515, 1573			Asymmetric C_α=C_β stretching
	1628		C-C in benzene ring (stretch)
	1610		C=C in quinone ring (stretch)
	1513		N-H bending
	1458, 1440		C=N and CH=CH (stretch)
	1359		C-N^+ polarons (stretch)
	1255		C-N in benzenoid ring (stretch)
	1140		C-H in semiquinone ring (bend)
	855		Benzenoid ring deformation in emeraldine salt
	815		Quinoid ring deformation
	608, 624		Benzenoid ring in-plane deformation
		984, 928	Ring deformation
		1105, 1066	Symmetrical C-H in plane bending
		1257	Asymmetrical C-H in plane bending
		1319, 1295	Asymmetrical C-N stretching
		1608	C=C stretching

of C-C in the aromatic ring (benzenoid-type) of PANI polymer [44, 45]. The PANI spectrum shows bands at 1610 cm^{-1} and 1513 cm^{-1} which correspond to the C=C stretching in the quinoid ring and N-H bending, respectively [45–47]. Two small bands at the positions 1458 cm^{-1} and 1420 cm^{-1} are ascribed to the C=N and C=C stretching in quinoid rings [48]. A band near 1359 cm^{-1} associated with the stretching of C-N^+ of radical cations in semiquinone form was observed [46, 48]. Furthermore, a band around 1255 cm^{-1} is attributed to C-N in-plane stretching in benzenoid rings [45, 48], whereas the vibration of C-H bending in semiquinone rings is seen at 1140 cm^{-1}. This vibration is due to the oxidized state (emeraldine) of the formed polymer [44]. Within the region 608 cm^{-1} to 855 cm^{-1}, the ring deformation and ring in-plane deformation bands for the benzenoid ring and quinoid ring were observed [48].

In the case of PPy films (Figure 4(c)), a band located at 1608 cm^{-1} is assigned as C=C backbone stretching, whereas both peaks at 1319 and 1295 cm^{-1} are originated from asymmetrical C-N stretching mode of the pyrrole ring. Furthermore, a peak positioned at the 1257 cm^{-1} is assigned to the asymmetrical C-H in-plane bending. As can be seen from the spectrum, the peak located at 1066 cm^{-1} is attributed to symmetrical C-H in-plane bending, while the bands for pyrrole ring deformation are seen at the positions 984 cm^{-1} and 926 cm^{-1}. The presence of the C-H in-plane deformation peak proved that oxidized PPy was successfully produced in this study [49]. A sharp peak at 926 and 1105 cm^{-1} is associated with in-plane deformation of the pyrrole bipolaron structure. In addition, the bands at the 984 cm^{-1} and 1066 cm^{-1} are related to the polaron pyrrole ring [50, 51].

The surface morphologies of the prepared polymer films were examined by scanning electron microscope (SEM). Different morphologies were observed (Figure 5) through electropolymerization of the monomers by varying the monomer concentration. The PEDOT polymer film obtained from the electrodeposition of 1 mM EDOT displays few bulges on the surface of ITO substrate (Figure 4(a)). In contrast, PEDOT film prepared from 5 mM exhibits few globular clusters aggregate together forming a thin layer of film. Both polymer films show a mixture of small and large nodules in which the ITO surface is not fully covered. Furthermore, the comparison between 5 mM (Figure 5(b)) and 10 mM (Figure 5(c)) PEDOT micrographs revealed that the nodules are merged together for 10 mM PEDOT film forming a compact layer thick layer and the globular clusters are distributed evenly on the substrate. There is an apparent observation on the structure of PEDOT film at lower magnification (inset Figure 5(c)) where it shows densely packed and smooth homogeneous film fully covering the electrode.

PANI films prepared from 1 mM ANI exhibit cylindrical-like shape (Figure 5(d)). However, as the concentration is increased to 5 mM, the morphology of the films shows loose discrete spherical particle with granular morphology (Figure 5(e)), while PANI prepared from 10 mM (Figure 5(f))

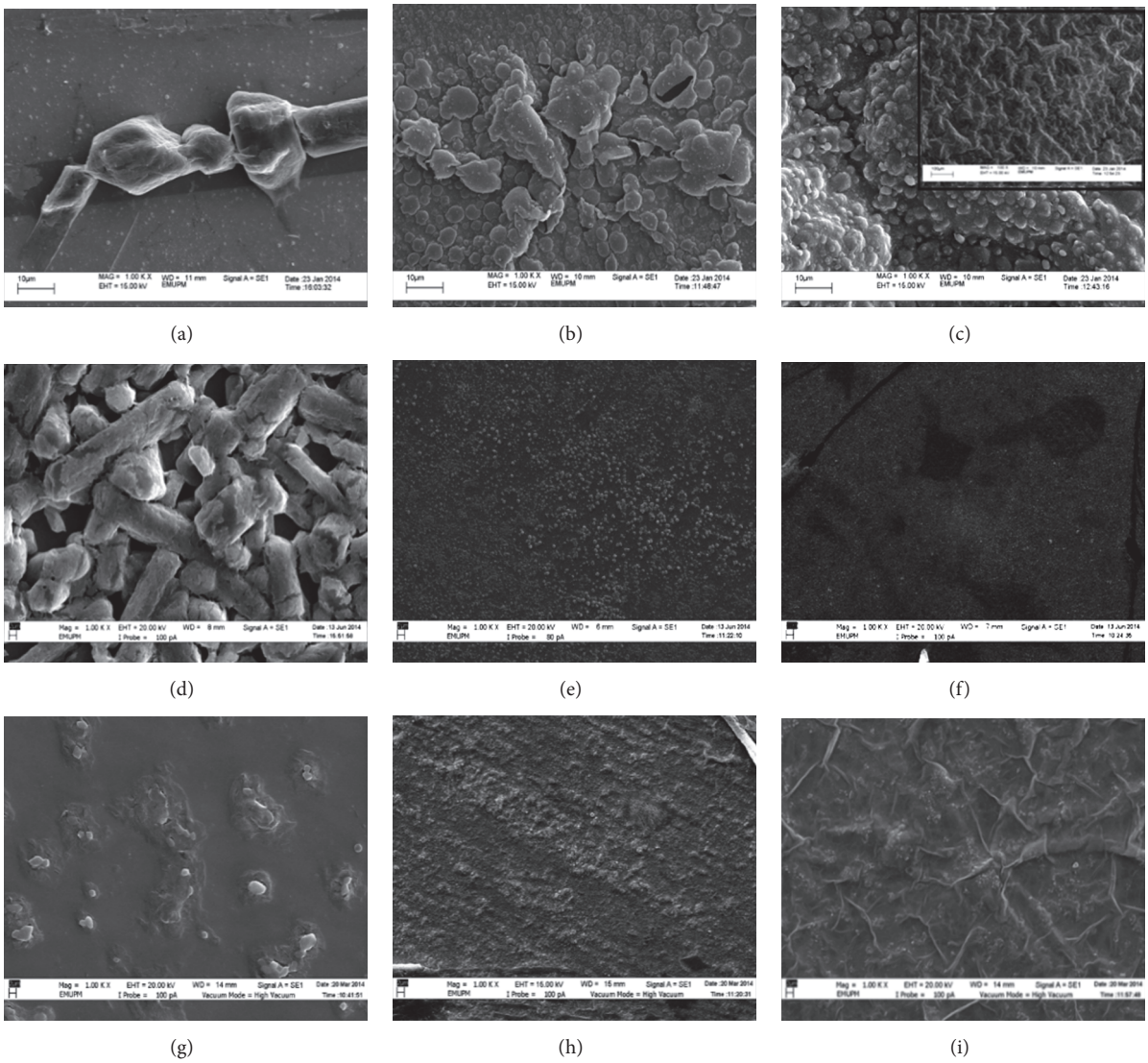

Figure 5: SEM micrographs of (a) 1 mM PEDOT, (b) 5 mM PEDOT, (c) 10 mM PEDOT, (d) 1 mM PANI, (e) 5 mM PANI, (f) 10 mM PANI, (g) 1 mM PPy, (h) 5 mM PPy, and (i) 10 mM PPy.

shows granular particles that are evenly distributed on the surface forming a uniform ordered morphology. Comparison among the PPy films prepared at different concentrations showed significant different morphology with each other, signifying the importance of the concentration on the electropolymerization process. The differences in morphology of PPy films are visible where 1 mM PPy exhibited few small bulges (Figure 5(g)) scattered all over the surface of the electrode. It is worth noticing that, at 1 mM, PPy film is not fully covered on the surface of the electrode. In contrast, 5 mM PPy and 10 mM PPy films revealed that both films have homogeneous surface morphology covering the whole electrode. However, 5 mM PPy shows grain structure (sand type morphology) (Figure 5(h)) while 10 mM PPy (Figure 5(i)) illustrates wrinkled surface morphology.

Therefore, the comparison of the SEM images between the polymers can be made; for example, 10 mM PEDOT, 10 mM PANI, and 10 mM PPy showed different morphologies even polymerized at the same concentration. Hence, the morphologies of the polymers could be controlled by varying the concentration of monomer to get the desired structures.

3.3. Electrochemical Properties

3.3.1. Cyclic Voltammetry. The capacitance properties of the prepared homopolymers were studied using cyclic voltammetry (CV). The specific capacitances values for the polymers were calculated according to

$$C = \frac{S}{\Delta U \times \upsilon \times A}, \quad (1)$$

where C is capacitance, S is the enclosed area in the CV curve, ΔU is the potential window, υ is the scan rate, and A is the area of the electrode.

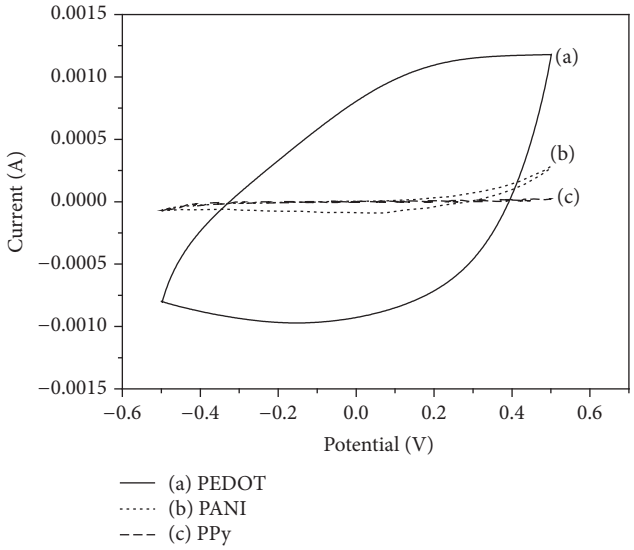

Figure 6: CVs of (a) PEDOT, (b) PANI, and (c) PPy films electropolymerized at from 10 mM monomer concentration recorded in 0.1 M KCl solution at the scan rate of 100 mV/s.

Figure 6 shows the typical CV curves of the homopolymers and the shapes are different from each other. However, the shape of CV for each homopolymer (PANI and PPy) is not varied significantly (Figure S2) as the concentration is increased except for the integrated area of the CV curves. Thus, the changes in the integrated area of the CV curves indicate the conducting polymers exhibit some differences in the electrochemical properties.

Generally, the ideal behaviour of electrical double layer (EDL) capacitor would display a rectangular shaped current-voltage curve (no reduction or oxidation peak) [52, 53]. However, the CV profiles in the present study did not exhibit any rectangular shaped curve. Thus, this implied that the synthesized polymers deviate from the pure ideal capacitor properties. The absence of redox peaks in the CVs indicates only the nonfaradaic reaction has occurred where deducing that the capacitive behaviour of the polymer films is based on the ion adsorption-desorption process at the interface of electrode and electrolyte without any chemical reaction [54].

As can be seen from the CV (Figure 6), PPy and PANI show oblique and narrow CV loop with a small integrated area of CVs, indicating large interfacial contact resistance of the film with bulk electrolyte and poor ionic propagation behaviour of the prepared polymer film [53, 55]. However, it is noticed that the CV of PEDOT (Figure 6(a)) displays a quasirectangular shape with the large integrated area and no apparent oxidation or reduction peaks, suggesting that the PEDOT-coated electrodes have excellent electrochemical double layer capacitances [56, 57]. This observation could be related to the structure of the PEDOT films layer with globular cluster surface morphologies that make the surface area higher and eventually increase the adsorption and desorption process. Additionally, it was observed that the specific capacitance values (Table 3) for all electropolymerized homopolymers are increasing with the increase monomer concentration. Notably, the lowest capacitance value was obtained for homopolymers prepared from 1 mM which could be due to the inhomogeneous and nonuniform film deposited on the substrate.

3.3.2. Electrochemical Impedance Spectroscopy (EIS) Measurements. The electrochemical impedance spectroscopy (EIS) is a useful and powerful method that is widely used to provide data on the electrochemical characteristics such as double layer capacitance, charge transfer resistance, diffusion impedance, and solution resistance [58, 59]. Impedance spectroscopy consists of a real component and imaginary component and they are measured as a function of the frequency. Generally, a small amplitude AC potential (sinusoidal form) is introduced to the system. The response is measured in the sinusoidal form at the same frequency but shifted in the phase. The Nyquist plot is one of the most used impedance spectra to understand the electrochemical responses.

The charge transfer characteristics of the homopolymers at different concentrations of the monomers were studied and the obtained impedance spectra are shown in Figure 7. Nyquist plots of PEDOT (Figure 7(a)) films include a semicircle at high-frequency region followed by a straight line indicating Warburg diffusion at the low-frequency region, whereas PANI (Figure 7(b)) exhibits two semicircles followed by a Warburg diffusion at low frequency. Nyquist plots of PPy exhibit similar pattern as PANI; however, the disappearance of Warburg element at the concentration of 5 mM is worth noticing and indicating poor ion diffusion from the bulk solution to the polymer surface, which could lead to high resistance of charge transfer. This electrochemical system can be modelled according to the equivalent circuits (Figure 8) which are used to fit the experimental data. The information obtained from the equivalent circuits is in agreement with the data interpreted from the Nyquist plots. The accuracy of the fitted data with the plot is determined based on the chi-square (χ^2) that represents the sum of the square of the differences between theoretical and experimental points and also limiting the percentage error in the value of each element in the equivalent circuits to a minimum [60]. The values of the χ^2 in the current work are in the range of 10^{-2} to 10^{-3}, indicating good fitting.

Three different equivalent circuits for the resultant homopolymers are proposed to investigate the electrochemical properties of the homopolymers (Figure 8). The equivalent circuits consist of the bulk solution resistance (R_s), charge transfer resistance between polymer coated electrode and electrolyte (R_{ct}), the resistance of the polymer film (R_p), constant phase element (CPE), and the "classical" infinite-length Warburg diffusion element (Z_W). The R_{ct} values can be calculated from the diameter of the semicircle obtained from the Nyquist plots [61]. In these models, CPE is used [62] in the circuits replacing the double layer capacitor, C_{dl} due to the nonhomogenous and irregular geometry morphologies of the homopolymers (as shown in the SEM images), CPE refers to the double layer capacitance and faradaic pseudocapacitance which express the nonideal behaviour of C_{dl} [63]. Additionally, it is worth noting that the Warburg element is

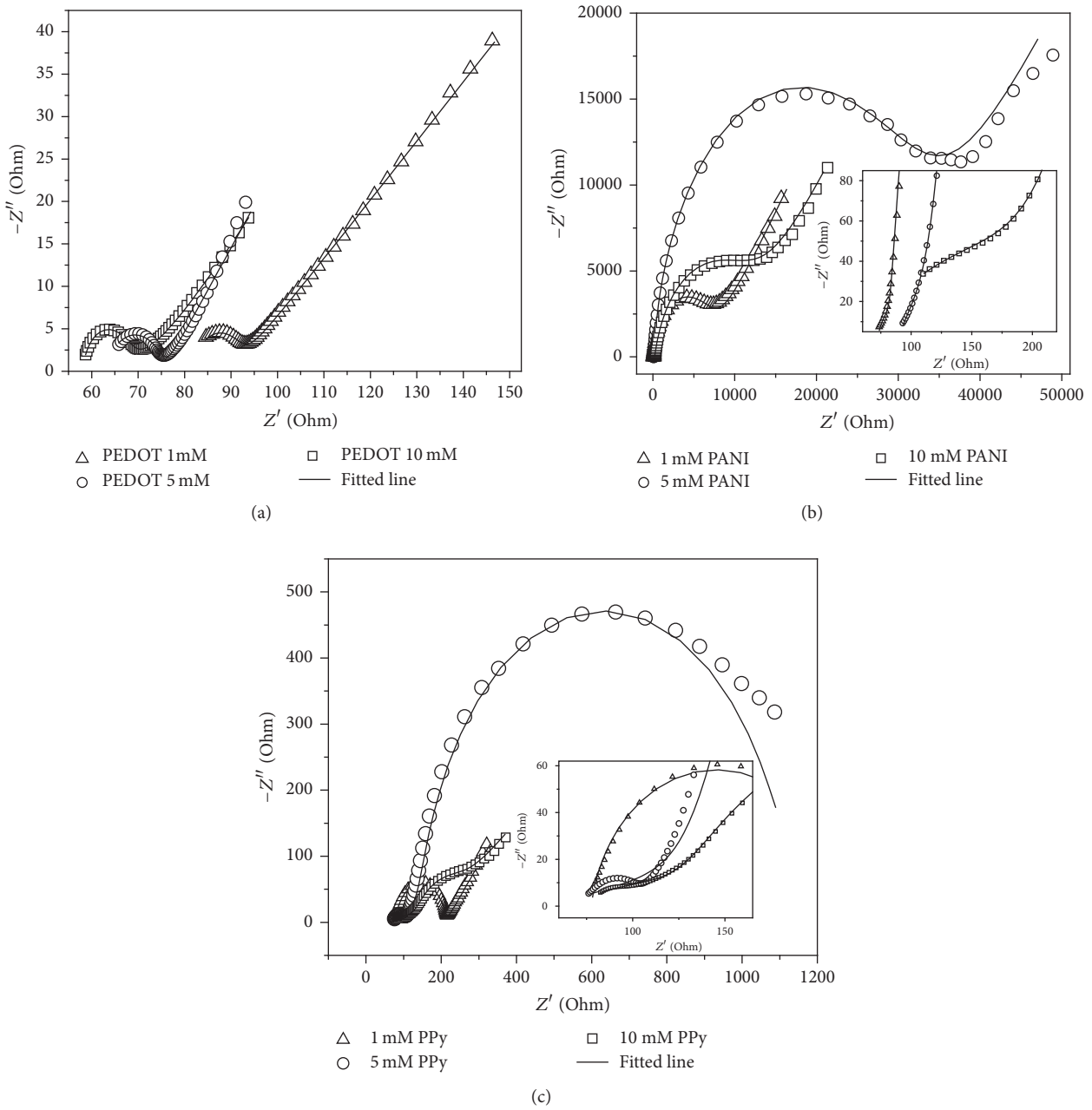

Figure 7: Nyquist plot of (a) PEDOT, (b) PANI, and (c) PPy deposited from the solution containing different monomer concentration on the ITO glass at 1.0 V. The solid lines represent the best fitting according to the equivalent circuits (Inset: magnification of Nyquist plot at high-frequency region).

Table 3: Electrochemical properties obtained from fitting data of Nyquist plots.

Concentration (mM)	PEDOT			PANI			PPy		
	C_{sp} (mF/cm^2)	R_{ct} (Ω)	χ^2 (10^{-3})	C_{sp} (mF/cm^2)	R_{ct} (Ω)	χ^2 (10^{-3})	C_{sp} (mF/cm^2)	R_{ct} (Ω)	χ^2 (10^{-3})
1 mM	0.54	9.26	0.22	0.06	6.88 k	20.61	0.01	134.50	11.14
5 mM	8.57	12.82	1.10	0.46	31.11 k	11.02	0.10	890.21	28.05
10 mM	12.8	21.72	5.67	0.62	11.85 k	8.50	0.11	103.11	2.91

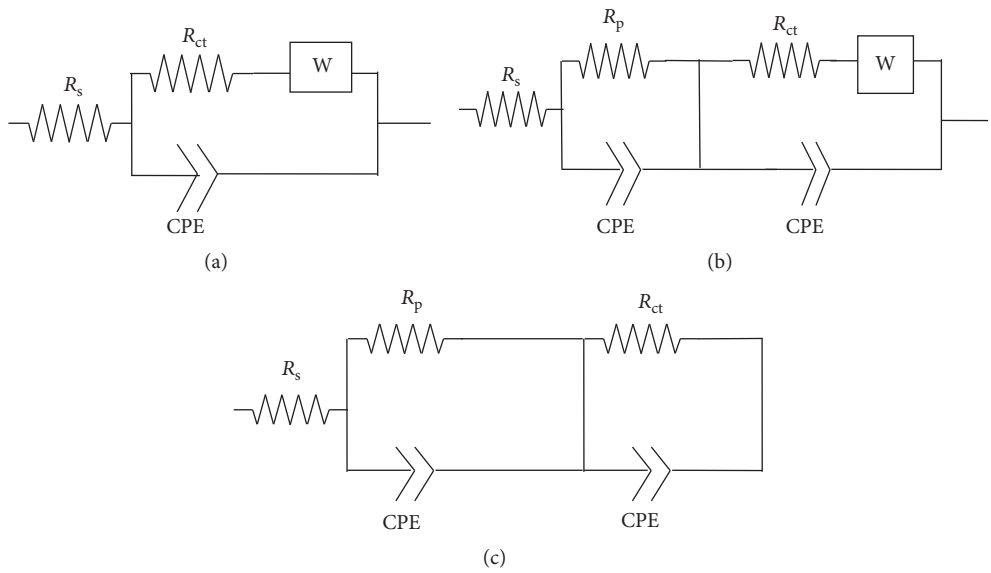

Figure 8: Equivalent circuits used in the fitting of the impedance results: (a) PEDOT, (b) PANI, 1 mM PPy and 10 mM PPy, and (c) 5 mM PPy.

not included in the circuits for PPy films except for 1 mM and 10 mM PPy film.

Based on Table 3, the R_{ct} values for PEDOT films increase with the increasing of monomer concentration. This phenomenon could be related to the morphology differences of the PEDOT. As can be seen from the SEM images of PEDOT (Figure 5), at 1 mM few bulges on the substrate were noticed and compact thick globular structures were obtained at 10 mM. The globular structure has a high surface area for ion adsorption-desorption process; however, the thicker layer slows down the process, which eventually increases the resistance for charge carriers.

The R_{ct} values for PANI and PPy increase with concentration (from 6.88 kΩ and 134.50 Ω at 1 mM to 31.11 kΩ and 890.21 Ω at 5 mM for PANI and PPy films, resp.) before decreasing at 10 mM. It is expected that the changes in the morphology have affected the charge transfer at the interface. At the concentration of 1 mM, PANI film exhibit cylindrical shaped structures and formed a loose discrete spherical particle with granular morphology at 5 mM (Figure 5(d)). However, when the concentration of ANI is increased to 10 mM, a film with compact granular particles was observed which improves the accessibility of the electrolyte and subsequently reduce the charge transfer. Similarly, in the case of PPy, at 1 mM the film shows small bulges morphology on the surface. When the concentration is increased to 5 mM Py and 10 mM Py, the films reveal grain structure (sand type structure) and compact layer with wrinkled surface morphology. It is expected that wrinkled surface provides more active sites for rapid ion diffusion which reduces the resistance of charge transfer.

The work carried out on polybenzidine by Muslim et al. [64] also showed that different monomer concentration affects the morphology, structure, and electrochemical activities which is consistent with results of the current study, whereas in another study conducted by Ates [65] revealed that the initial monomer concentration influenced the capacitive properties of poly(3-methylthiophene).

4. Conclusion

Comparison of PEDOT, PANI, and PPy polymer films on the effect of concentration was presented in this work. FTIR and Raman spectra confirm the presence of polymers on ITO substrate. SEM analysis revealed significant differences in morphologies of the polymers as the concentration is increased. The polymers electropolymerized from 10 mM monomer solution display a homogenous formation of the film. The differences in the polymer morphologies prepared from different concentrations eventually affect the electrochemical properties.

Competing Interests

The authors declare that there is no conflict of interests regarding the publication of this paper.

Acknowledgments

This work was supported by a Universiti Putra Malaysia research grant (no. GP-IPS/2013/9399838)

References

[1] H. Shirakawa, E. J. Louis, A. G. MacDiarmid, C. K. Chiang, and A. J. Heeger, "Synthesis of electrically conducting organic polymers: halogen derivatives of polyacetylene, $(CH)_x$," *Journal of the Chemical Society, Chemical Communications*, no. 16, pp. 578–580, 1977.

[2] H. Shirakawa, "The discovery of polyacetylene film: the dawning of an era of conducting polymers (Nobel Lecture)," *Angewandte Chemie—International Edition*, vol. 40, no. 14, pp. 2575–2580, 2001.

[3] K. Cysewska, J. Karczewski, and P. Jasiński, "Influence of electropolymerization conditions on the morphological and electrical properties of PEDOT film," *Electrochimica Acta*, vol. 176, Article ID 25282, pp. 156–161, 2015.

[4] L. Groenendaal, F. Jonas, D. Freitag, H. Pielartzik, and J. R. Reynolds, "Poly(3,4-ethylenedioxythiophene) and its derivatives: past, present, and future," *Advanced Materials*, vol. 12, no. 7, pp. 481–494, 2000.

[5] S. Kulandaivalu, Z. Zainal, and Y. Sulaiman, "A New Approach for Electrodeposition of poly (3, 4-ethylenedioxythiophene)/polyaniline (PEDOT/PANI)Copolymer," *International Journal of Electrochemical Science*, vol. 10, no. 11, pp. 8926–8940, 2015.

[6] D. S. Patil, S. A. Pawar, J. H. Kim, P. S. Patil, and J. C. Shin, "Facile preparation and enhanced capacitance of the Ag-PEDOT:PSS/polyaniline nanofiber network for supercapacitors," *Electrochimica Acta*, vol. 213, pp. 680–690, 2016.

[7] D. S. Patil, S. A. Pawar, J. Hwang, J. H. Kim, P. S. Patil, and J. C. Shin, "Silver incorporated PEDOT: PSS for enhanced electrochemical performance," *Journal of Industrial and Engineering Chemistry*, vol. 42, pp. 113–120, 2016.

[8] M. S. Ahmed, H. Jeong, J.-M. You, and S. Jeon, "Synthesis and characterization of an electrochromic copolymer based on 2,2′:5′,2″-terthiophene and 3,4-ethylenedioxythiophene," *Applied Nanoscience*, vol. 2, no. 2, pp. 133–141, 2012.

[9] H. J. Ahonen, J. Lukkari, and J. Kankare, "n- and p-doped poly(3,4-ethylenedioxythiophene): two electronically conducting states of the polymer," *Macromolecules*, vol. 33, no. 18, pp. 6787–6793, 2000.

[10] S. K. Dhawan, D. Kumar, M. K. Ram, S. Chandra, and D. C. Trivedi, "Application of conducting polyaniline as sensor material for ammonia," *Sensors and Actuators B: Chemical*, vol. 40, no. 2-3, pp. 99–103, 1997.

[11] D. Geethalakshmi, N. Muthukumarasamy, and R. Balasundaraprabhu, "Measurement on the structural, morphological, electrical and optical properties of PANI-CSA nanofilms," *Measurement*, vol. 92, pp. 446–452, 2016.

[12] M. Jaymand, "Recent progress in chemical modification of polyaniline Dedicated to Professor Dr. Ali Akbar Entezami.," *Progress in Polymer Science*, vol. 38, no. 9, pp. 1287–1306, 2013.

[13] S. Bhadra, D. Khastgir, N. K. Singha, and J. H. Lee, "Progress in preparation, processing and applications of polyaniline," *Progress in Polymer Science*, vol. 34, no. 8, pp. 783–810, 2009.

[14] H. Kawashima and H. Goto, "Preparation and properties of polyaniline in the presence of trehalose," *Soft Nanoscience Letters*, vol. 1, no. 3, pp. 71–75, 2011.

[15] L. Ma, L. Su, J. Zhang et al., "A controllable morphology GO/PANI/metal hydroxide composite for supercapacitor," *Journal of Electroanalytical Chemistry*, vol. 777, pp. 75–84, 2016.

[16] Y. Wei, J. Tian, and D. Yang, "A new method for polymerization of pyrrole and derivatives," *Die Makromolekulare Chemie, Rapid Communications*, vol. 12, no. 11, pp. 617–623, 1991.

[17] P. Saville, *Polypyrrole, Formation and Use*, Defence Research and Development Atlantic Dartmouth, Dartmouth, Canada, 2005.

[18] N. Li, D. Shan, and H. Xue, "Electrochemical synthesis and characterization of poly(pyrrole-co-tetrahydrofuran) conducting copolymer," *European Polymer Journal*, vol. 43, no. 6, pp. 2532–2539, 2007.

[19] R. A. Jeong, G. J. Lee, H. S. Kim, K. Ahn, K. Lee, and K. H. Kim, "Physicochemical properties of electrochemically prepared polypyrrole perchlorate," *Synthetic Metals*, vol. 98, no. 1, pp. 9–15, 1998.

[20] T. Patois, B. Lakard, S. Monney, X. Roizard, and P. Fievet, "Characterization of the surface properties of polypyrrole films: Influence of electrodeposition parameters," *Synthetic Metals*, vol. 161, no. 21-22, pp. 2498–2505, 2011.

[21] K. M. Ziadan and W. T. Saadon, "Study of the electrical characteristics of polyaniline prepeared by electrochemical polymerization," *Energy Procedia*, vol. 19, pp. 71–79, 2012.

[22] X. Meng, Z. Wang, L. Wang, M. Pei, W. Guo, and X. Tang, "Electrosynthesis of pure poly(3,4-ethylenedioxythiophene) (PEDOT) in chitosan-based liquid crystal phase," *Electronic Materials Letters*, vol. 9, no. 5, pp. 605–608, 2013.

[23] T. Darmanin and F. Guittard, "Superhydrophobic surface properties with various nanofibrous structures by electrodeposition of PEDOT polymers with short fluorinated chains and rigid spacers," *Synthetic Metals*, vol. 205, pp. 58–63, 2015.

[24] M. Gerard, A. Chaubey, and B. D. Malhotra, "Application of conducting polymers to biosensors," *Biosensors and Bioelectronics*, vol. 17, no. 5, pp. 345–359, 2002.

[25] Z. Qi and P. G. Pickup, "High performance conducting polymer supported oxygen reduction catalysts," *Chemical Communications*, no. 21, pp. 2299–2300, 1998.

[26] J. Zang, Y. Wang, X. Zhao et al., "Electrochemical synthesis of polyaniline on nanodiamond powder," *International Journal of Electrochemical Science*, vol. 7, no. 2, pp. 1677–1687, 2012.

[27] A. Kellenberger, D. Ambros, and N. Plesu, "Scan rate dependent morphology of polyaniline films electrochemically deposited on nickel," *International Journal of Electrochemical Science*, vol. 9, no. 12, pp. 6821–6833, 2014.

[28] Y. Xiao, X. Cui, J. M. Hancock, M. Bouguettaya, J. R. Reynolds, and D. C. Martin, "Electrochemical polymerization of poly(hydroxymethylated-3,4-ethylenedioxythiophene) (PEDOT-MeOH) on multichannel neural probes," *Sensors and Actuators B: Chemical*, vol. 99, no. 2-3, pp. 437–443, 2004.

[29] S. Sadki and C. Chevrot, "Electropolymerization of 3,4-ethylenedioxythiophene, N-ethylcarbazole and their mixtures in aqueous micellar solution," *Electrochimica Acta*, vol. 48, no. 6, pp. 733–739, 2003.

[30] N. Sakmeche, S. Aeiyach, J.-J. Aaron, M. Jouini, J. C. Lacroix, and P.-C. Lacaze, "Improvement of the electrosynthesis and physicochemical properties of poly(3,4-ethylenedioxythiophene) using a sodium dodecyl sulfate micellar aqueous medium," *Langmuir*, vol. 15, no. 7, pp. 2566–2574, 1999.

[31] L. Pigani, A. Heras, Á. Colina, R. Seeber, and J. López-Palacios, "Electropolymerisation of 3,4-ethylenedioxythiophene in aqueous solutions," *Electrochemistry Communications*, vol. 6, no. 11, pp. 1192–1198, 2004.

[32] H. Randriamahazaka, V. Noël, and C. Chevrot, "Nucleation and growth of poly(3,4-ethylenedioxythiophene) in acetonitrile on platinum under potentiostatic conditions," *Journal of Electroanalytical Chemistry*, vol. 472, no. 2, pp. 103–111, 1999.

[33] S. Patra, K. Barai, and N. Munichandraiah, "Scanning electron microscopy studies of PEDOT prepared by various electrochemical routes," *Synthetic Metals*, vol. 158, no. 10, pp. 430–435, 2008.

[34] S. Bijani, R. Schrebler, E. A. Dalchiele, M. Gabás, L. Martínez, and J. R. Ramos-Barrado, "Study of the nucleation and growth

mechanisms in the electrodeposition of micro- and nanostructured Cu_2O thin films," *The Journal of Physical Chemistry C*, vol. 115, no. 43, pp. 21373–21382, 2011.

[35] G. Shumakovich, G. Otrokhov, I. Vasil'eva, D. Pankratov, O. Morozova, and A. Yaropolov, "Laccase-mediated polymerization of 3,4-ethylenedioxythiophene (EDOT)," *Journal of Molecular Catalysis B: Enzymatic*, vol. 81, pp. 66–68, 2012.

[36] Y.-J. Tao, H.-F. Cheng, W.-W. Zheng, Z.-Y. Zhang, and D.-Q. Liu, "Electrosynthesises and characterizations of copolymers based on pyrrole and 3,4-ethylenedioxythiophene in aqueous micellar solution," *Synthetic Metals*, vol. 162, no. 7-8, pp. 728–734, 2012.

[37] C. Li and T. Imae, "Electrochemical and Optical Properties of the Poly(3,4- ethylenedioxythiophene) film electropolymerized in an aqueous sodium dodecyl sulfate and lithium tetrafluoroborate medium," *Macromolecules*, vol. 37, no. 7, pp. 2411–2416, 2004.

[38] K. Zhang, J. Xu, X. Zhu et al., "Poly(3,4-ethylenedioxythiophene) nanorods grown on graphene oxide sheets as electrochemical sensing platform for rutin," *Journal of Electroanalytical Chemistry*, vol. 739, pp. 66–72, 2015.

[39] N.-A. Rangel-Vazquez, C. Sánchez-López, and F. R. Felix, "Spectroscopy analyses of polyurethane/polyaniline IPN using computational simulation (Amber, MM+ and PM3 method)," *Polímeros*, vol. 24, no. 4, pp. 453–463, 2014.

[40] A. Kellenberger, E. Dmitrieva, and L. Dunsch, "The stabilization of charged states at phenazine-like units in polyaniline under p-doping: an in situ ATR-FTIR spectroelectrochemical study," *Physical Chemistry Chemical Physics*, vol. 13, no. 8, pp. 3411–3420, 2011.

[41] F. F. Bruno, S. A. Fossey, S. Nagarajan, R. Nagarajan, J. Kumar, and L. A. Samuelson, "Biomimetic synthesis of water-soluble conducting copolymers/homopolymers of pyrrole and 3,4-ethylenedioxythiophene," *Biomacromolecules*, vol. 7, no. 2, pp. 586–589, 2006.

[42] S. Cetiner, H. Karakas, R. Ciobanu et al., "Polymerization of pyrrole derivatives on polyacrylonitrile matrix, FTIR-ATR and dielectric spectroscopic characterization of composite thin films," *Synthetic Metals*, vol. 160, no. 11-12, pp. 1189–1196, 2010.

[43] S. Garreau, J. L. Duvail, and G. Louarn, "Spectroelectrochemical studies of poly(3,4-ethylenedioxythiophene) in aqueous medium," *Synthetic Metals*, vol. 125, no. 3, pp. 325–329, 2001.

[44] R. Mažeikiene, G. Niaura, and A. Malinauskas, "Chemical oxidation of aniline and N-methylaniline: a kinetic study by Raman spectroscopy," *Spectrochimica Acta Part A: Molecular and Biomolecular Spectroscopy*, vol. 106, pp. 34–40, 2013.

[45] U. Bogdanović, V. V. Vodnik, S. P. Ahrenkiel, M. Stoiljković, G. Ćirić-Marjanović, and J. M. Nedeljković, "Interfacial synthesis and characterization of gold/polyaniline nanocomposites," *Synthetic Metals*, vol. 195, pp. 122–131, 2014.

[46] M. Jain and S. Annapoorni, "Raman study of polyaniline nanofibers prepared by interfacial polymerization," *Synthetic Metals*, vol. 160, no. 15-16, pp. 1727–1732, 2010.

[47] K. A. Ibrahim, "Synthesis and characterization of polyaniline and poly(aniline-co-o-nitroaniline) using vibrational spectroscopy," *Arabian Journal of Chemistry*, 2013.

[48] T. Lindfors and A. Ivaska, "Raman based pH measurements with polyaniline," *Journal of Electroanalytical Chemistry*, vol. 580, no. 2, pp. 320–329, 2005.

[49] Y. Furukawa, S. Tazawa, Y. Fujii, and I. Harada, "Raman spectra of polypyrrole and its 2,5-^{13}C-substituted and C-deuterated analogues in doped and undoped states," *Synthetic Metals*, vol. 24, no. 4, pp. 329–341, 1988.

[50] M. Li, J. Yuan, and G. Shi, "Electrochemical fabrication of nanoporous polypyrrole thin films," *Thin Solid Films*, vol. 516, no. 12, pp. 3836–3840, 2008.

[51] J. Duchet, R. Legras, and S. Demoustier-Champagne, "Chemical synthesis of polypyrrole: structure-properties relationship," *Synthetic Metals*, vol. 98, no. 2, pp. 113–122, 1998.

[52] B. E. Conway, "Capacitance behavior of films of conducting, electrochemically reactive polymers," in *Electrochemical Supercapacitors: Scientific Fundamentals and Technological Applications*, pp. 299–334, Springer, Berlin, Germany, 1999.

[53] P. Si, S. Ding, X.-W. Lou, and D.-H. Kim, "An electrochemically formed three-dimensional structure of polypyrrole/graphene nanoplatelets for high-performance supercapacitors," *RSC Advances*, vol. 1, no. 7, pp. 1271–1278, 2011.

[54] C.-W. Liew, S. Ramesh, and A. K. Arof, "Characterization of ionic liquid added poly(vinyl alcohol)-based proton conducting polymer electrolytes and electrochemical studies on the supercapacitors," *International Journal of Hydrogen Energy*, vol. 40, no. 1, pp. 852–862, 2015.

[55] B. E. Conway, "Electrochemical supercapacitors," in *Scientific Fundamentals and Technological Applications*, Springer, Berlin, Germany, 1999.

[56] W. Chen, R. B. Rakhi, and H. N. Alshareef, "High energy density supercapacitors using macroporous kitchen sponges," *Journal of Materials Chemistry*, vol. 22, no. 29, pp. 14394–14402, 2012.

[57] X. Feng, N. Chen, Y. Zhang et al., "The self-assembly of shape controlled functionalized graphene-MnO_2 composites for application as supercapacitors," *Journal of Materials Chemistry A*, vol. 2, no. 24, pp. 9178–9184, 2014.

[58] B. E. Conway, J. O. M. Bockris, R. White et al., "Electrochemical impedance spectroscopy and its applications," in *Modern Aspects of Electrochemistry*, Modern Aspects of Electrochemistry, pp. 143–248, Springer, Berlin, Germany, 2002.

[59] M. Ates, "Review study of electrochemical impedance spectroscopy and equivalent electrical circuits of conducting polymers on carbon surfaces," *Progress in Organic Coatings*, vol. 71, no. 1, pp. 1–10, 2011.

[60] S. Chaudhari and P. P. Patil, "Inhibition of nickel coated mild steel corrosion by electrosynthesized polyaniline coatings," *Electrochimica Acta*, vol. 56, no. 8, pp. 3049–3059, 2011.

[61] N. F. Atta, A. Galal, and R. A. Ahmed, "Poly(3,4-ethylene-dioxythiophene) electrode for the selective determination of dopamine in presence of sodium dodecyl sulfate," *Bioelectrochemistry*, vol. 80, no. 2, pp. 132–141, 2011.

[62] C.-C. Hu and C.-H. Chu, "Electrochemical impedance characterization of polyaniline-coated graphite electrodes for electrochemical capacitors—effects of film coverage/thickness and anions," *Journal of Electroanalytical Chemistry*, vol. 503, no. 1-2, pp. 105–116, 2001.

[63] W.-C. Chen, T.-C. Wen, and A. Gopalan, "Negative capacitance for polyaniline: an analysis via electrochemical impedance spectroscopy," *Synthetic Metals*, vol. 128, no. 2, pp. 179–189, 2002.

[64] A. Muslim, D. Malik, and A. A. Rexit, "Effects of monomer concentration on the structure and properties of polybenzidine micro rods," *Polymer Science Series B*, vol. 54, no. 11, pp. 518–524, 2012.

[65] M. Ates, "Monomer concentration effects of poly (3-methylthiopene) on electrochemical impedance spectroscopy," *International Journal of Electrochemical Science*, vol. 4, no. 7, pp. 1004–1014, 2009.